

Antibacterial and photocatalytic performance of Silver orthophosphate/Hydroxyapatite composite

Ahmed Elyacoubi ^{1,*}, Amine Rkhaila ², Brahim sallek ³ and Brahim Chafik El idrissi ¹

¹ Chemical Team Materials Surfaces Interfaces, Laboratory Materials and Energetics, Fac of Sciences, Ibn Tofail University, kenitra, B.P: 133, Kénitra, Morocco

² Laboratory of nutrition, health and environment; Applied microbiology team. Ibn Tofail University. Morocco

³ Agroressources and process engineering laboratory, Ibn Tofail University, Kénitra, Morocco

Abstract: The present work reports the synthesis of pure hydroxyapatite and HAp supported Ag₃PO₄ (Ag₃PO₄/HAp composites) with varying amounts of silver ions Ag⁺ with a facile in-situ ion exchange method. XRD results of Ag₃PO₄/HAp composite reveal the peaks characteristic of pure HAp with additional peaks of silver ions which suggest the deposit of silver particles on the support surface (HAp). The nano-composites Ag₃PO₄/HAp samples show good adsorption and improved photocatalytic activities in methylene blue MB degradation (more than 70%). Antibacterial study of Ag₃PO₄/HAp nano-composites showed that the HAp dried at 90°C possesses some antibacterial activity against Escherichia coli and Staphylococcus aureus bacteria. Also, compared to HAp sample, deposition of Ag₃PO₄ nanoparticles on HAp surface improves the antibacterial performance of the composites.

Keywords: Hydroxyapatite; silver orthophosphate; Gram-positive and Gram-negative bacteria; photodegradation.

Introduction

Nowadays, the textile industries and photographic industries reject vast quantities of polluted wastewater. The purification of water from chemical products and microbial contaminations has become a great environmental challenge. Semiconductor-based photocatalysis seems to be a promising and efficient material to decompose pollutants substances using solar light. Among many photocatalysts, titanium oxide (TiO₂) is widely used thanks to its high photocatalytic activity and chemical stability ¹. Unfortunately, TiO₂ shows good photocatalytic activity only under ultraviolet (UV) (<387nm) ², which limits its use as a photocatalytic material. Therefore, it is necessary to look for other possible alternative photocatalysts to TiO₂. Ag₃PO₄ was recently found as an alternative photocatalyst material for solar photocatalysis, which can oxidize water and decompose organic dye with excellent photo-oxidation activity ³. The photodegradation performance of Ag₃PO₄ was found to be higher than that of other classical photocatalysts such as N-TiO₂ and BiVO₄ ^{4,5}. Umezawa and co-workers studied the origin of high photocatalytic performance using the density functional theory based on the first principles calculations indicating that Ag₃PO₄ had a large

dispersion of conduction band facilitating the separation of electron/hole pairs (e⁻/h⁺) ⁶.

However, Silver phosphate can be reduced to metallic silver Ag⁰ during the photodegradation reaction. Also, the photoinduced electron (e⁻) cannot react with O₂ to form O₂^{-•} because the conduction band CB position is more positive than that red/ox potential of O₂/O₂^{-•} (E°=-0.33V) ⁷. Therefore, the photoinduced electrons cannot be combined with O₂ to form reduction products, which is necessary for the photodegradation process. To enhance the performance of photoinduced electrons for Ag₃PO₄ material various methods have been adopted by coupling and constructing a heterogeneous junction between Ag₃PO₄ and another semiconductor supports such as Ag₃PO₄/TiO₂ ⁸, Ag₃PO₄/Graphene oxide ⁹ and Ag₃PO₄/SnO₂ ¹⁰. Due to its properties such as biocompatibility, bioactivity and biodegradability, Hydroxyapatite HAp, with chemical formula Ca₁₀(PO₄)₆(OH)₂, is a potential candidate to be used as catalyst support and as a support for inorganic antibacterial agents. HAp supported Ag₃PO₄ proves to be a promising material for visible light activated photocatalyst.

*Corresponding author : Ahmed Elyacoubi
Email address : elyacoubi6ahmed@gmail.com
DOI: <http://dx.doi.org/10.13171/mjc841906173ae>

Received February 11, 2019
Accepted June 1, 2019
Published June 17, 2019

On the other hand, HAp particles could be contaminated by bacteria during the synthesis or implantation stage. It has been noticed that the HAp does not present any antibacterial activity which limits its use as implant ¹¹. However, Tin-Oo et al. ¹² reported that HAp possesses some antibacterial activity with the broth dilution technique. Hence, the improvement of HAp antibacterial activity has become essential and necessary to ensure the implantation of the HAp biomaterial without any bacterial infections. In this regard, one of the ways to improve the antibacterial activity of HAp is using metal ions to minimize the risk of bacterial contaminations and therefore prevent the growth of pathogens on the implant surface. Various metal ions such as Ag^+ , Zn^{2+} or Cu^{2+} can be used in the coating of the implant to eliminate the bacterial adhesion and growth ^{13, 14}. One of these ions, which present an excellent antibacterial activity, is Ag^+ thanks to its substantial toxicity property towards a broad range of pathogens ¹⁵. Ag^+ ions are also very well known for their antibacterial properties and non-toxic characteristics to human cells at low quantities. The cytotoxicity of Ag^+ might be due to size, the shape of particles and also to their accumulation inside human cells, leading to their dysfunctions ¹⁶. So, coupling the Ag_3PO_4 and HAp proves to be useful and beneficial to enhance the antibacterial activity of implants if they are used in feeble concentrations.

The present work aims to synthesize the nano-composites of HAp supported Ag_3PO_4 with varying amounts through a facile in-situ ion exchange method as well as silicon-substituted HAp (SixHAp) by the wet chemical precipitation method. The synthesized nano-composites were analysed by XRD technique. In order to understand the effect of the support on the Ag_3PO_4 photocatalysis, the photodegradation of MB under visible light irradiation was investigated. The effect of Ag_3PO_4 deposited on HAp surface on the antibacterial activity of HAp was studied through disk diffusion method by measuring the zone inhibition for each sample against *Escherichia coli* (*E. coli*) and *Staphylococcus aureus* (*S. aureus*).

Materials and methods

Synthesis of samples

Pure Hydroxyapatite (HAp), as a support, was synthesized via conventional aqueous precipitation method as it was briefly dealt in our previous paper ¹⁷. Briefly, 0.925g of calcium hydroxide $\text{Ca}(\text{OH})_2$ was dissolved in 25ml of deionized water DI and stirring for 15min at room temperature. Concurrently, 0.720g of phosphoric acid (H_3PO_4) was dissolved in 25ml of DI water and stirring for 15min and added drop by drop, under stirring, to the already prepared solution of $\text{Ca}(\text{OH})_2$. The pH of the slurry remained higher than 10 (no ammonia was added). The resultant mixture was stirred for 2h and then matured over 48h

at ambient temperature. The as-prepared precipitate was filtered and dried at 90°C for 24h.

The Ag_3PO_4 nanoparticles were prepared by the liquid-solid method, and 0.408g of silver nitrate (Riedel-de Haën, 98.5-100%) directly added under stirring to 20ml of an already prepared $(\text{NH}_4)_2\text{HPO}_4$ (LOBA CHEMIE) solution (5.4g/L). After 2h of agitation, the resulting paste was filtered and dried at 80°C for 12h. On the other hand, to synthesize $\text{Ag}_3\text{PO}_4/\text{HAp}$ nano-composites, 0.5g of the biomaterial supports (HAp) was added to 20ml of DI water and aged for 10min. Then, 15ml of nitrate silver precursor, containing the desired quantity of AgNO_3 (0.05, 0.1 and 0.15g), was mixed with HAp precursor and kept under stirring for 4h at room temperature and matured over 12h. The yellow product suspensions were removed by filtration, and the remaining particles were dried at 80°C for 12h to remove the residual water. For reference, the samples were labelled as $\text{Ag}_3\text{PO}_4/\text{HAp}$ -1 with 5.8% (weight percentage) of Ag, $\text{Ag}_3\text{PO}_4/\text{HAp}$ -2 (10.6 wt.% of Ag) and $\text{Ag}_3\text{PO}_4/\text{HAp}$ -3 (14.6 wt.% of Ag) and the amount of AgNO_3 added is 0.05g 0.1g and 0.15g respectively.

Powders characterization

The identification of crystallites phases of all samples was investigated by Philips X'Pert PRO X-ray diffractometer (XRD) using $\text{CuK}\alpha$ radiation ($\lambda = 1.5406 \text{ \AA}$) at 40 kV and 30 mA. The XRD patterns were collected in the 2θ range of 10–60° with a step of 0.02°. The morphological characteristics of as-synthesized nanoparticles were carried out by scanning electron microscopy (SEM, Hitachi, S-3400N).

Photocatalytic measurements

The as-prepared photocatalysts were evaluated through the photodegradation of the MB organic pollutant in aqueous solution under visible light irradiation (36W LED lamp). 50 mg of each photocatalyst was dispersed into 50ml MB solution dye (20mg/l), and then the result suspensions were stirred in the dark for 30min to establish adsorption-desorption equilibrium between MB and photocatalysts. After irradiation time, the MB aqueous solution was sampled and centrifuged to eliminate the photocatalysts. The remaining concentration of MB was measured using a UV-vis spectrophotometer (Jenway, Serial: 67XX) and the decolorization efficiency (%) was calculated by the following equation (1):

$$\text{Decolorization (\%)} = (C/C_0) \times 100\% = (A/A_0) \times 100\%$$

Where C_0 and A_0 were the initial concentration and initial absorbance of MB respectively, while C and A were the concentration and absorbance after the irradiation of visible light respectively.

In an attempt to understand the effect of the silver percentage on the antibacterial activity compared to HAp as a control, the antibacterial properties were carried out against two kinds of bacteria strain: Staphylococcus sharp and intense peaks indicate the high purity (S. aureus) and Escherichia coli (E. coli) as Gram-positive and Gram-negative strains, respectively. The used pathogens were isolated from the nutrition, health and environment laboratory; by the microbiology team, at Ibn Tofail University in Morocco. The test evaluation is performed by the disk diffusion method. The disks of filter paper (Woltman n°1); with a diameter of 5mm; emerged for 24h in the solutions containing the samples already sterilized by tyndallization (at 60 °C over 30 min then 5-10 °C over

30 min). The diffusion technique was performed using the Müller-Hinton Agar (MHA). The zone plates were carried out by filling the used agar into Petri dishes, then 1cm³ of the 10⁸ (cfu cm⁻³) suspension of each tested species was poured and spread over the MHA medium previously prepared simple (the bacterial culture was 24 hours old). The as-prepared disks (already emerged) were deposited on the medium culture and incubated for 24h at 37°C. The culture of the blank sample investigated in the same conditions, and the same nutrient broth medium is used for all tests. All of the tests were repeated ten times, and their average represented the results. The obtained results were performed by measuring the width of the inhibition zone (cm).

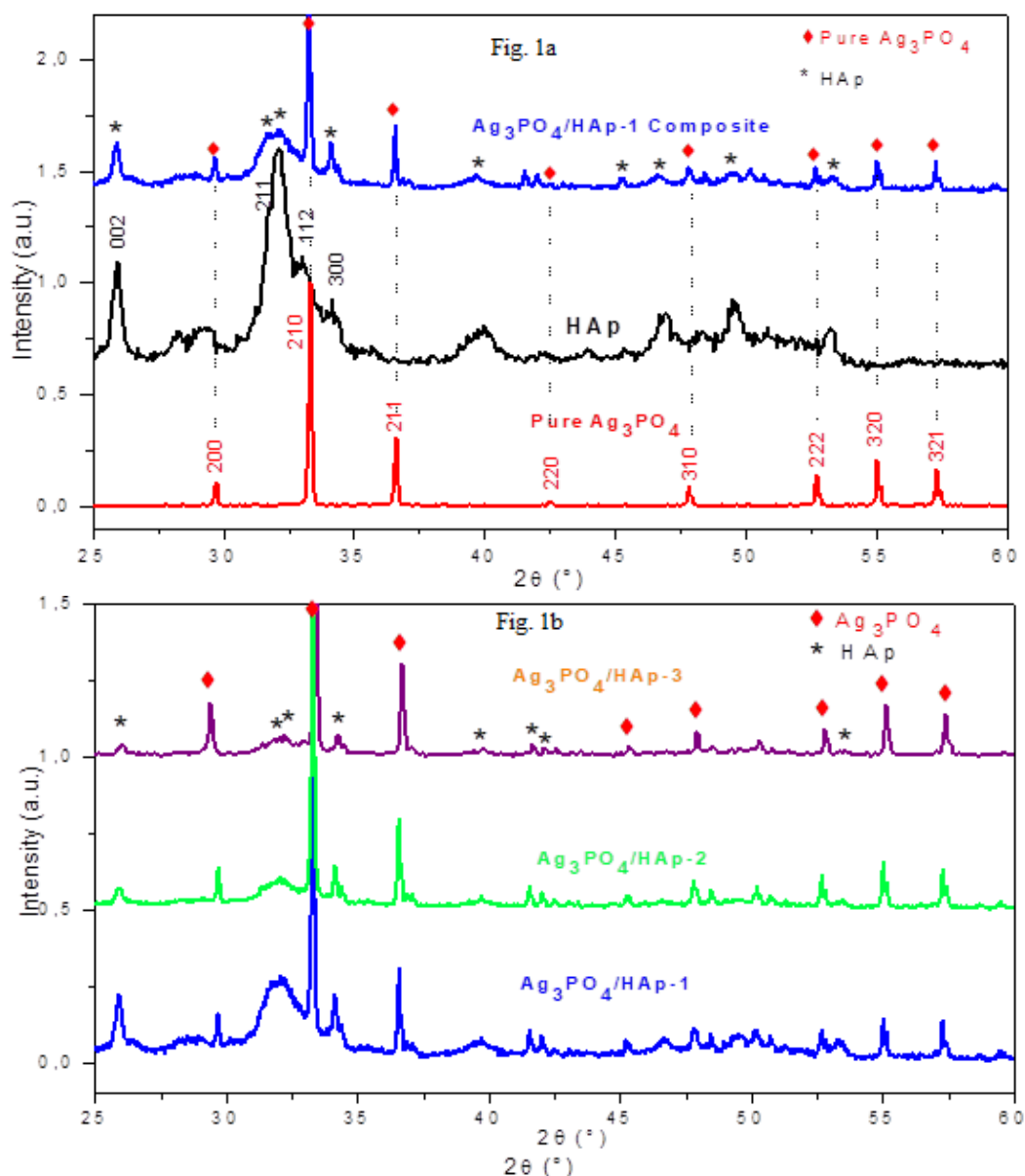


Figure 1. XRD diffraction data of (a) HAp support, pure Ag₃PO₄, Ag₃PO₄/HAp-1 and (b) Ag₃PO₄/HAp-1, Ag₃PO₄/HAp-2 and Ag₃PO₄/HAp-3 composites

Results and discussion

Characterization of products

The phase and the crystallinity of resultant products were investigated by XRD diffraction analysis. Figure 1 shows the XRD patterns of samples. Fig 1-a represents the XRD patterns of pure hydroxyapatite support (HAp) dried at 90°C, pure Ag₃PO₄ and Ag₃PO₄/HAp-1 composite. Fig 1-b shows just the XRD patterns of three composites samples.

All XRD patterns were indexed based on JCPDS card n° 06-505 for Ag₃PO₄ and JCPDS Card n° 9-432 for hydroxyapatite support Ca₁₀(PO₄)₆(OH)₂. The important diffraction peaks characteristics of HA apatite were observed located at 25.89° - 32.13° - 33.00 and 34.15° corresponding to (002), (211), (112) and (300) planes, respectively¹⁸. XRD pattern of pure HAp did not show the presence of any other materials as a secondary phase. The broad peaks of pure HAp reveal the presence of a significant amount of amorphous phase, which is in good accordance with the literature¹⁸. On the other side, the eight peaks located at 29.77°, 33.39°, 36.65°, 42.50°, 47.82°, 52.71°, 55.06° and 57.30° correspond to the (200), (210), (211), (220), (310), (222), (320) and (321) planes of pure Ag₃PO₄ nanoparticles, respectively¹⁹.

Therefore, the sharp and intense peaks indicate the high crystallinity and crystallinity of Ag₃PO₄ particles. Lattice parameters and crystallite size of the synthesized Ag₃PO₄ particles were calculated using the Full Prof program and Scherrer equation, respectively. The mean estimated crystallite size and lattice parameters were 0.56 Å, and a=6.0139 Å, respectively and the structure of Ag₃PO₄ microcrystal was determined as a body-centred cubic structure with P-43n space group (JCPDS no 06-0505). Thus the XRD analysis reveals also that the as-prepared sample of silver nitrate is pure Ag₃PO₄ with no detected impurities phases. After impregnation of metallic silver, all composites samples show both the peaks characteristic of HAp and Ag₃PO₄, suggesting the successful deposit of Ag₃PO₄ microcrystals on the HAp support surface and confirming their coexistence. As the amount of AgNO₃ increase, the characteristic peaks of Ag₃PO₄ nano-crystals become increasingly intense.

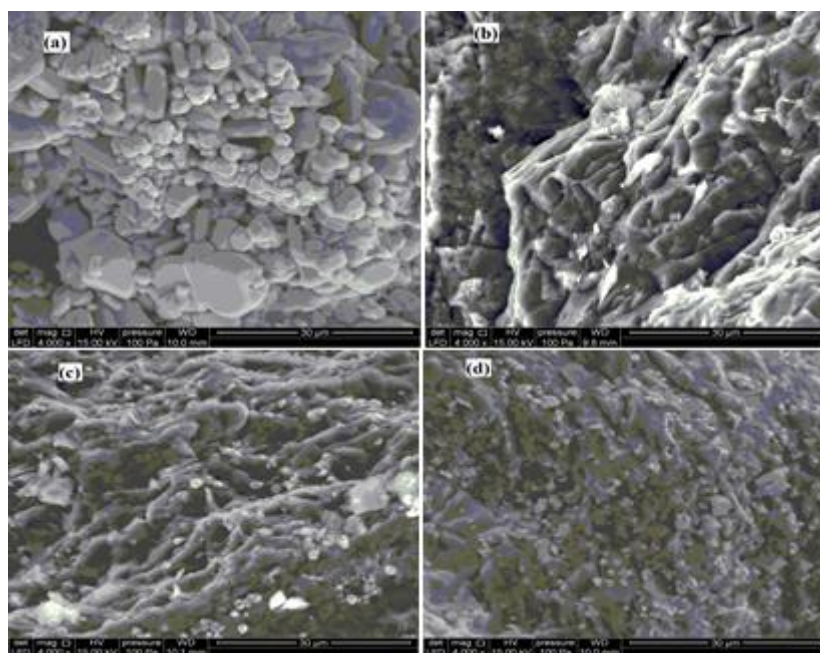


Figure 2. SEM images of (a) Ag₃PO₄, (b) Ag₃PO₄/Hap-1, (c) Ag₃PO₄/Hap-2 and (d) Ag₃PO₄/Hap-3

The mean crystallite size (L) of Ag₃PO₄ particles was calculated from the XRD data using the Scherrer equation as follow (2):

$$L = \frac{k\lambda}{\beta \cos \theta}$$

Where L = crystallite size, K = the shape factor equal to 0.9, λ = wavelength of Cu Kα radiation equal to 1.5406 Å, θ = half of the diffraction angle and

β = full width at half maximum (FWHM), the Scherrer equation is relative to a single peak (210).

The morphologies of as-prepared photocatalysts were characterized by scanning electron microscopy (SEM), and the representative images are shown in Figure 2. It can be seen that the Ag₃PO₄ nanoparticles exhibit both a nanorod and irregular polyhedra morphologies with a smooth surface (Fig 2.a).

The particles size varies than from 1.5 to 9 microns (Fig 2.a). In Fig 2.b-d, we can see the numerous bright particles with a mean particle size of 1–2.5 microns are deposited onto the surface of the support (dark surface) suggesting the deposition of Ag_3PO_4 nano-particles on HAp surface. Based on the above SEM images, we can infer that the use of hydroxyapatite support promotes better dispersion and enhances stronger contact with Ag_3PO_4 . Hence, the anti-agglomeration of Ag_3PO_4 nanoparticles can be realized in the samples, which is favourable to the reduction of the particle size of Ag_3PO_4 and therefore beneficial to the photocatalytic process.

Figure 3 shows the photocatalytic performance of as-prepared samples to decompose MB dye after exposing to visible light irradiation. The decolorization of MB dye was measured by absorbance at 664 nm which is largely taken as a

reference to evaluate the decolorization rate of MB organic dye. Furthermore, the absorbance of MB at 291nm could be used to extract information about the degradation stage of the entire dye²⁰. For the HAp sample, and according to Figure 3, it can be seen that the MB concentration remains practically unchanged under visible light irradiation in 120min. In addition, the pure Ag_3PO_4 photocatalyst exhibits very good photocatalytic activity under visible irradiation, and 98% of MB is decomposed after 60min reaction time. The photocatalytic activity of Ag_3PO_4 particles depends on the balance between the size and morphology. Xiang et al reported that the Ag_3PO_4 nanorods exhibit good photocatalytic activity for dye degradation. Obviously, the good photocatalytic activity can be explained by the nanorod and irregular polyhedra morphology of pure Ag_3PO_4 nano-particles.

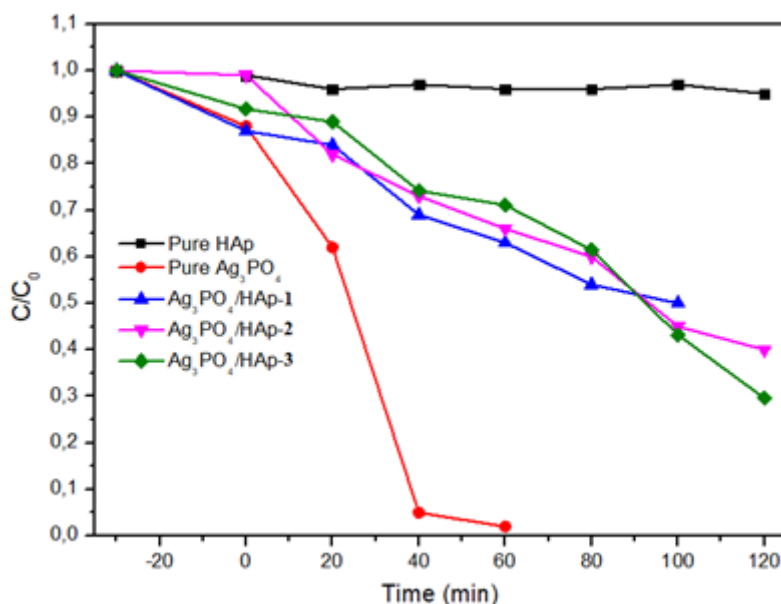


Figure 3. degradation curves for MB using HAp, Pure Ag_3PO_4 , $\text{Ag}_3\text{PO}_4/\text{HAp-1}$, $\text{Ag}_3\text{PO}_4/\text{HAp-2}$ and $\text{Ag}_3\text{PO}_4/\text{HAp-3}$

Compared with pure HAp, the $\text{Ag}_3\text{PO}_4/\text{HAp}$ nano-composites show a superior photodegradation rate of MB, which was due to the deposited Ag_3PO_4 ²¹. It should also be noted that the photocatalytic activity of $\text{Ag}_3\text{PO}_4/\text{HAp}$ composites increase when the concentration of silver ions increase. Under visible irradiation, $\text{Ag}_3\text{PO}_4/\text{HAp-3}$ show higher photocatalytic performance compared to other silver hydroxyapatite composites with a decolorization rate of MB of 70.30% in 120min. However, the decolorization rate of $\text{Ag}_3\text{PO}_4/\text{HAp-1}$ and $\text{Ag}_3\text{PO}_4/\text{HAp-2}$ are only 50% and 55% in 100min respectively. We can observe that the decolorization rate of $\text{Ag}_3\text{PO}_4/\text{HAp-1}$ and $\text{Ag}_3\text{PO}_4/\text{HAp-2}$ is higher than that of $\text{Ag}_3\text{PO}_4/\text{HAp-3}$ until 100 min and vice versa at 120min. Moreover, a small amount of silver ion could improve the photocatalytic activity due to

the slow release of deposited silver ions on the HAp support by photogenerated electrons which leads to the rapid carrier (electrons and holes) separation under visible light irradiation²².

Antibacterial assessment

The antibacterial activities of HAp, pure Ag_3PO_4 and $\text{Ag}_3\text{PO}_4/\text{HAp}$ samples were investigated by measuring the zone inhibition (ZoI) against *E. coli* and *S. aureus* strains (Table 1). The antibacterial efficiency of the test is evaluated by measuring the diameter of ZoI around the disk. When the ZoI increases the antibacterial efficiency becomes more critical. Results show that the samples have acted differently on the two bacteria. According to the obtained results, it can be seen that the *E. coli* strain is less responsive than *S. aureus* ones to all studied

compounds (Figure 4). This difference in response might be due to the difference in the cellular wall

structure of Gram-positive and Gram-negative strain^{23,24}.

Table 1. Average diameter (cm) of zone inhibition.

SAMPLES	E. Coli	S. aureus
Hydroxyapatite support	0.85 [a]	1 [ab]
Ag ₃ PO ₄ microcrystals	1.1 [c]	1.25 [ab]
Ag ₃ PO ₄ /HAp-1	1 [c]	1.15 [ab]
Ag ₃ PO ₄ /HAp-2	1.1 [b]	1.25 [ab]
Ag ₃ PO ₄ /HAp-3	1.4 [d]	1.5 [ab]

The same letter means that the samples do not differ significantly at the 5% threshold.

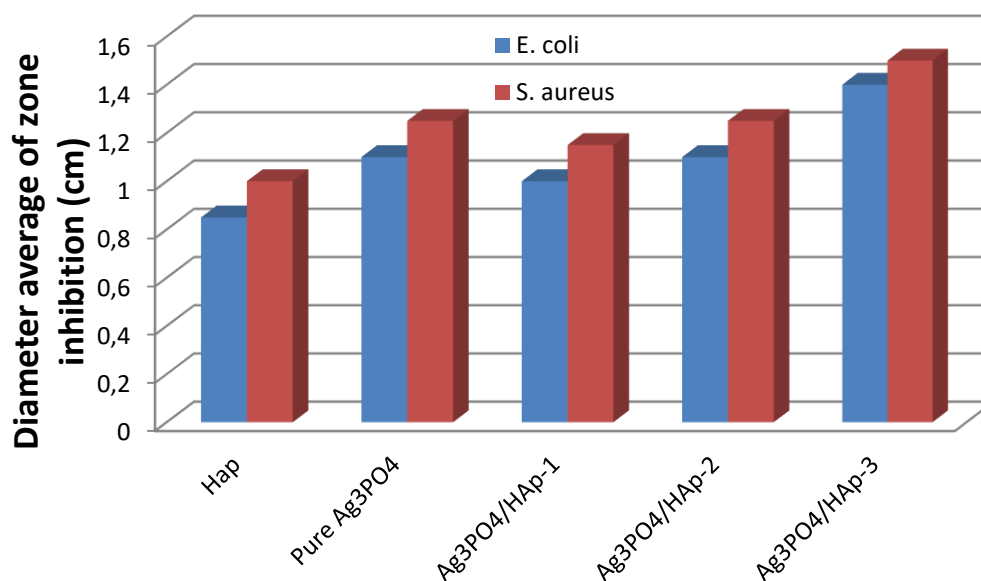


Figure 4. histograms of diameter average of zone inhibition of as-prepared samples.

A. Z. Alshemary²⁵ et al. and N. Iqbal et al.²⁶ reported that the HAp has no antibacterial effect against E. coli bacteria strain using the disk diffusion method while Archan et al.¹¹ found that there is no antibacterial activity against S. aureus using the same method. According to Tin O-o study¹², the HAp microcrystals possess antibacterial activity using the broth dilution technique. In the present study, it can be seen that the HAp support acted differently and it presents a low antibacterial activity against both bacteria strain. The zones inhibition for E. coli and S. aureus were 0.85 and 1.00 cm respectively. Moreover, the E. coli bacteria are less affected by antimicrobial agent Ag₃PO₄ than S. aureus. In the literature, Ag₃PO₄ is well known for its antibacterial property. The silver ions release around the disk kill the pathogens and thus limit the growth of microorganisms.

On the other hand, the ZoI was observed for three HAp supported Ag₃PO₄ samples against E. coli and S. aureus strains. The average inhibition zones increase when the percentage of Ag ions increases for two studied pathogens. The average ZoI of Ag₃PO₄/HAp-

1, Ag₃PO₄/HAp-2 and Ag₃PO₄/HAp-3 for E. coli were 1, 1.1 and 1.4 cm respectively. Ag₃PO₄/HAp-1, Ag₃PO₄/HAp-2 and Ag₃PO₄/HAp-3 showed zone inhibition of 1.15, 1.25 and 1.5 cm toward S. aureus. Our results are in good accordance with the authors who studied the effect of silver ions Ag⁺ on E. coli and S. aureus^{23, 27-31}. The antibacterial properties of silver ions Ag⁺ were ascribed to the high surface/volume ratio of silver particles, which gives more efficiency and enhances their antibacterial activity³².

Feng et al. and Song et al. suggested the mechanism explaining the influence of the silver ions on cell bacteria^{33, 34}. The Ag⁺ ions attack the bacterium proteins at its cell wall causing cellular problems and then separate the cytoplasm from the bacterial cell wall. The silver ions may attach to bacterial DNA and RNA and thus prevents bacterial replication leading finally to the death of the cell. Mocanu et al.³⁵ report that the silver ions attack preferably the respiratory chain and cell division.

Conclusion

Nano-hydroxyapatite HAp and Ag_3PO_4 supported hydroxyapatite $\text{Ag}_3\text{PO}_4/\text{HAp}$ were successfully synthesized. XRD data of HAp reveal the diffraction peaks typical of pure HAp apatite. The diffraction spectra of $\text{Ag}_3\text{PO}_4/\text{HAp}$ composites show the coexistence of HAp phase and silver ions. Also, coupling Ag_3PO_4 with hydroxyapatite support reveals a high photocatalytic activity to decompose methylene blue MB dye comparing to pure HAp. Antibacterial tests show that the $\text{Ag}_3\text{PO}_4/\text{HAp}$ particles have good antibacterial activity against *E. coli* and *S. aureus* strains. Consequently, our composites mainly $\text{Ag}_3\text{PO}_4/\text{HAp}$, could be used in dental and surgical applications as a bone implant or coating metallic implants.

References

- 1- K. Hashimoto, H. Irie, et A. Fujishima, TiO_2 Photocatalysis: A Historical Overview and Future Prospects, *Jpn. J. Appl. Phys.*, vol 44, no 12, **2005**, 8269-8285.
- 2- J.-M. Herrmann, Photocatalysis fundamentals revisited to avoid several misconceptions, *Appl. Catal. B Environ.*, vol. 99, no 3-4, **2010**, 461-468.
- 3- Z. Yi, J. Ye, N. Kikugawa, T. Kako, S. Ouyang, H. Stuart-Williams, H. Yang, J. Cao, W. Luo, Z. Li, Y. Liu, R.L. Withers, *Nat. Mater* 9, **2010**, 559-564.
- 4- R. Asahi, Visible-Light Photocatalysis in Nitrogen-Doped Titanium Oxides, *Science*, vol. 293, no 5528, **2001**, 269-271.
- 5- Weerasak Chomkitichai, Jiraporn Pama, Pimchanok Jaiyen, Sila Pano, Jiraporn Ketwaraporn, Pusit Pookmanee, Sukon Phanichphant and Pongthep Jansanthea, *Applied Mechanics and Materials*, **2019**, 886, 138-145.
- 6- N. Umezawa, O. Shuxin, et J. Ye, Theoretical study of high photocatalytic performance of Ag_3PO_4 , *Phys. Rev. B*, vol. 83, no 3, **2011**, 035202-1-8.
- 7- X. Fu, W. Tang, L. Ji, et S. Chen, $\text{V}_2\text{O}_5/\text{Al}_2\text{O}_3$ composite photocatalyst: Preparation, characterization, and the role of Al_2O_3 , *Chem. Eng. J.* vol. 180, **2012**, 170-177.
- 8- W. Yao, B. Zhang, C. Huang, C. Ma, X. Song, et Q. Xu, Synthesis and characterization of high efficiency and stable $\text{Ag}_3\text{PO}_4/\text{TiO}_2$ visible light photocatalyst for the degradation of methylene blue and rhodamine B solutions, *J. Mater. Chem.*, vol. 22, no 9, **2012**, 4050.
- 9- H. Cui et al., Facile synthesis of graphene oxide-enwrapped Ag_3PO_4 composites with highly efficient visible light photocatalytic performance, *Mater. Lett.*, vol. 93, **2013**, 28-31.
- 10- L. Zhang, H. Zhang, H. Huang, Y. Liu, et Z. Kang, $\text{Ag}_3\text{PO}_4/\text{SnO}_2$ semiconductor nanocomposites with enhanced photocatalytic activity and stability, *New J. Chem.*, vol. 36, no 8, **2012**, 1541.
- 11- Archan Rajendran, Rakesh C. Barik, Duraipandy Natarajan, M.S. Kiran, Deepak K. Pattanayak, Synthesis, phase stability of hydroxyapatite–silver composite with antimicrobial activity and cytocompatibility, *Ceramics International* 40, **2014**, 10831-10838.
- 12- M.M. Tin-Oo, V. Gopalakrishnan, A.R. Samsuddin, K.A. Al Salihi, et O. Shamsuria, Antibacterial property of locally produced hydroxyapatite, *Arch. Orof. Sci.* 2, **2007**, 41-44.
- 13- W. Chen, Y. Liu, H.S. Courtney, M. Bettenga, C.M. Agrawal, J.D. Bumgardner, J.L. Ong, In vitro anti-bacterial and biological properties of magnetron co-sputtered silver-containing hydroxyapatite coating, *Biomaterials* 27, **2006**, 5512-5517.
- 14- R.J. Chung, M.F. Hsieh, C.W. Huang, L.H. Perng, H.W. Wen, T.S. Chin, Antimicrobial effects and human gingival biocompatibility of hydroxyapatite sol-gel coatings, *J. Biomed. Mater. Res. Part B* 76, **2006**, 169-178.
- 15- R.W. Sun, R. Chen, N.P. Chung, C.M. Ho, C.L. Lin, C.M. Che, Silver nanoparticles fabricated in Hepes buffer exhibit cytoprotective activities toward HIV-1 infected cells, *Chem. Commun.* 40, **2005**, 5059-5061.
- 16- Wen-Ru. Li, Xiao-Bao. Xie, Qing-Shan. Shi, Hai-Yan. Zeng, You-Sheng OU-Yang, Yi-Ben. Chen, Antibacterial activity and mechanism of silver nanoparticles on *Escherichia coli*, *Appl Microbiol Biotechnol*, **2010**, 1115-1122.
- 17- B. Chafik El Idrissi, K. Yamni, A. Yacoubi, A. Massit, A novel method to synthesize nanocrystalline hydroxyapatite: Characterization with x-ray diffraction and infrared spectroscopy, *IOSR Journal of Applied Chemistry*. Volume 7, Issue 5, Ver. III, **2014**, 107-112.
- 18- J.J. Buckley, A.F. Lee, L. Olivi, K. Wilson, Hydroxyapatite supported antibacterial Ag_3PO_4 nanoparticles, *Journal of Materials Chemistry* 20, **2010**, 8056-8063.
- 19- Gopal Panthi, Rosa Ranjit, Hak-Yong Kim, Deependra Das Mulmi, Size-dependent optical and antibacterial properties of Ag_3PO_4 synthesized by facile precipitation and colloidal approach in aqueous solution, *Optik* 156, **2018**, 60-68.
- 20- X. Ma et al., Substantial change in the phenomenon of “self-corrosion” on $\text{Ag}_3\text{PO}_4/\text{TiO}_2$ compound photocatalyst, *Appl. Catal. B Environ.*, vol. 158-159, **2014**, 314-320.
- 21- Y. Bi, S. Ouyang, N. Umezawa, J. Cao, et J. Ye, Facet Effect of Single-Crystalline Ag_3PO_4

- 4 Sub-microcrystals on Photocatalytic Properties, *J. Am. Chem. Soc.*, vol. 133, no 17, **2011**, 6490-6492.
- 22- Xiaoting Hong, Xiaohui Wu, Qiuyun Zhang, Mingfeng Xiao, Gelin Yang, Meirong Qiu, Guocheng Han, Hydroxyapatite supported Ag₃PO₄ nanoparticles with higher visible light photocatalytic activity, *Applied Surface Science* 258, **2012**, 4801-4805.
- 23- V. Stanic, S. Dimitrijevic', J. Antic-Stankovic', M. Mitric', B. Jokic', Ilija B. Plecas', S. Raicevic', Synthesis, characterization and antimicrobial activity of copper and zinc-doped hydroxyapatite nanopowders, *Applied Surface Science* 256, **2010**, 6083-6089.
- 24- E. Amato, Y.A. Diaz-Fernandez, A. Taglietti, P. Pallavicini, L. Pasotti, L. Cucca, C. Milanese, P. Grisoli, C. Dacarro, J.M. Fernandez-Hechavarria, V. Necchi, Synthesis, characterization and antibacterial activity against Gram positive and Gram negative bacteria of biomimetically coated silver nanoparticles, *Langmuir* 27, **2011**, 9165-9173.
- 25- Ammar Z. Alshemary, Muhammed Akram, Yi-Fan Goh, Usman Tariq, Faheem K. Butt, Ahmad Abdolahi, Rafaqat Hussain, Synthesis, characterization, in vitro bioactivity and antimicrobial activity of magnesium and nickel doped silicate hydroxyapatite, *Ceramics International* 41, **2015**, 11886-11898.
- 26- Nida Iqbal, Mohammed Rafiq Abdul Kadir, Nik Ahmad Nazim Nik Malek, Nasrul Humaimi Bin Mahmood, Malliga Raman Murali, T. Kamarul, Characterization and antibacterial properties of stable silver substituted hydroxyapatite nanoparticles synthesized through surfactant assisted microwave process, *Materials Research Bulletin* 48, **2013**, 3172-3177.
- 27- M. Diaz, F. Barba, M. Miranda, F. Guitian, R. Torrecillas, J.S. Moya, Synthesis, antimicrobial activity of silver-hydroxyapatite nanocomposite, *J. Nanomater*, 2009, Article ID 498505.
- 28- L.F. de Oliveira, J.O. de Gonçalves, A. Kaliandra, J. Kobarg, M.B. Cardoso, Sweeter but deadlier: decoupling size, charge and capping effects in carbohydrate coated bactericidal silver nanoparticles, *J. Biomed. Nanotechnol.* 9, **2013**, 18171826.
- 29- W.R. Li, X.B. Xie, Q.S. Shi, S.S. Duan, Y.S. Ouyang, Y.B. Chen, Antibacterial effect of silver nanoparticles of *Staphylococcus aureus*, *Biometals* 24, **2011**, 135-141.
- 30- S. Cavalu, V. Simon, G. Goller, I. Akin, Bioactivity and antimicrobial proprieties of PMMA/Ag₂O acrylic bone cement collagen coated Dig. *J. Nanomater. Bios.* 6, **2011**, 779-790.
- 31- M. Bellantone, H.D. Williams, L.L. Hench, Broad-spectrum bactericidal activity of Ag₂O-doped bioactive glass, *Antimicrob. Agents Chemother.* 46, **2002**, 1940-1945.
- 32- Raffi, M., Hussain, F., Bhatti, T.M., Akhter, J.I., Hameed, A., Hasan, M.M, Antibacterial characterization of silver nanoparticles against *E. coli* ATCC-15224, *Journal of Materials Science and Technology* Volume 24, Issue 2, **2008**, 192-196.
- 33- H.Y. Song, K.K. Ko, I.H. Oh, B.T. Lee, Fabrication of silver nanoparticles and their antimicrobial mechanisms, *Eur. Cells. Mater.* 11, **2006**, 58.
- 34- Q.L. Feng, J. Wu, G.Q. Chen, F.Z. Cui, T.N. Kim, J.O. Kim, A mechanistic study of the antibacterial effect of silver ions on *Escherichia coli* and *Staphylococcus aureus*, *J. Biomed. Mater. Res. A* 52, **2000**, 662-668.
- 35- A. Mocanu, G. Furtos, S. Rapuntean, O. Horovitz, C. Flore, C. Garbo, A. Danisteanu, G. Rapuntean, C. Prejmerean, M. Tomoaia-Cotisel, Synthesis characterization and antimicrobial effects of composites based on multi-substituted hydroxyapatite and silver nanoparticles, *Applied Surface Science* 298, **2014**, 225-235.